

Selective sensitivity in Kerr microscopy

I. V. Soldatov and R. Schäfer

Based on conventional magneto-optical Kerr microscopy technique we have developed a new realization for the contrast separation of the in-plane and out-of-plane components of the surface magnetization. Utilizing the light from eight ultra-bright LED, guided to the microscope and been switched synchronously with the camera exposure, the domain images with pure in-plane magnetization can be obtained. We demonstrate the advantage of this new method various examples including NdFeB polycrystal and Cobalt single crystal. Moreover, such a technique was shown to strongly enhance the ultimate sensitivity of the magneto-optical microscopy by eliminating the parasitic contrast contribution, occurring in conventional experiments. The extreme accuracy was derived from optical hysteresis loops measured in $\text{Ni}_{81}\text{Fe}_{19}$ film and was shown to be as high as 0.6 mdeg.

I. INTRODUCTION

The wide-field Kerr effect microscopy since its introduction become a widely-used and effective tool for magnetic domain imaging^{1,2}. It provides the easy and direct access to the basic physical properties in macro- or nanoscales of magnetic devices of vital need for spintronic³⁻⁵ and spin caloritronic⁶⁻⁸. Particularly, if it is combined with other complimentary integral measurement techniques, like magnetometry or transport measurements, the knowledge of the magnetic microstructure gives a consummate insight into the origin of the magnetization reversal and the related processes.

All this has promoted the development of the the wide-field Kerr effect microscopy, and yet mainly in improving lateral or temporal resolution^{9,10}. The light sources have also been improved: the high-pressure mercury arc and xenon-arc lamps, which were in very regular use nowadays are ousted by the high-power LEDs, demonstrating the outstanding stability interchangeably with high luminosity and extremely long lifetime [link?]. Additionally, the great advancement in digital image processing were done: via the difference-imaging technique all non-magnetic features are eliminated, promoting the remaining domain contrast¹¹.

In spite of this improvements, the basic experimental principles of the Kerr microscopy and -magnetometry remains strait. It utilizes the magneto-optical Kerr effect, based on the interaction of the linearly polarized light with a magnetic media, which leads effectively to the rotation of the polarization plane of the incident light clockwise or counterclockwise depending on the orientation of the magnetization in the media. Due to this the reflected light (Kerr rotation) can be transformed to a domain contrast by placing an analyzer in the light path. Depending on the mutual orientation of the polarization plane, incident angle and magnetization direction in the specimen *polar* (the magnetization in media is out-of-plane), *longitudinal* (the magnetization is in-plane and at the same time in in plane of the incidence) and *transversal* (the magnetization is in-plane but transversal to the incidence plane) Kerr effects are distinguishable¹. And if *polar* is strongest when the angle of incidence is $\vartheta_0 = 0^\circ$ (the light is falling perpendicular on the surface), *lon-*

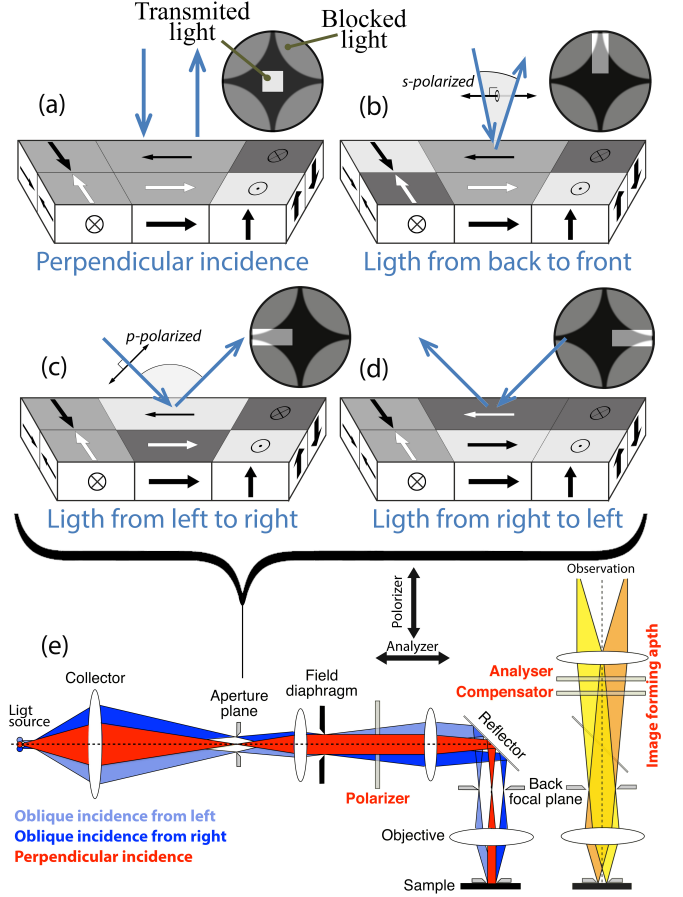


FIG. 1. The illustration of the contrast in the image of the magnetic sample: polar contrast (a), longitudinal with s-polarized light (b), longitudinal in transverse direction with p-polarized light with direct (c) and inverted contrast (d). The sketch of the Kerr microscope (e) with displaceable slit aperture, used for adjustment of the sensitivity.

gitudinal and *transversal* appear only for the light with non zero incident angle ($\vartheta_0 \neq 0^\circ$).

The most commonly used magneto-optical effects in Kerr microscopy are the polar and longitudinal Kerr effects. A sketch of the corresponding geometry is presented in Fig. 1. For the light coming to the sample surface at 90° only the polar contrast exists, and, thus, only

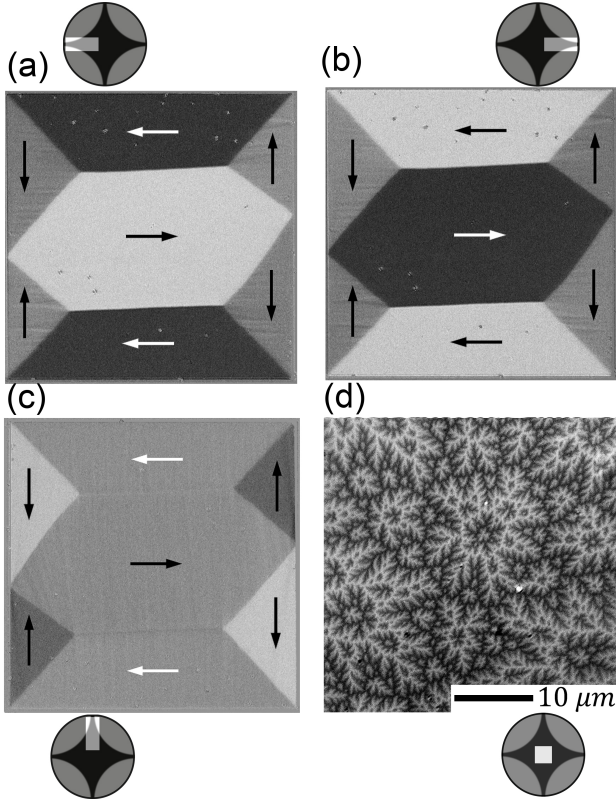


FIG. 2. **a-c**: magnetic domains in $\text{Ni}_{81}\text{Fe}_{19}$ (permalloy) thin (240 nm) patterned film elements taken in longitudinal sensitivity with p-polarized light. The contrast with the light coming from the left (**a**) is opposite to that with the light coming from the right (**b**). The side length of the element is $120\ \mu\text{m}$. **d**: out-of-plane magnetic domains in YIG ($\text{Y}_3\text{Fe}_2(\text{FeO}_4)_3$) film, obtained in polar sensitivity.

out-of-plane domains can be distinguished (Fig. 1 a). For non-zero angle of incidence two longitudinal Kerr contrasts are possible: i) when light polarization is in plane of incidence (*p*-polarization) then *longitudinal* contrast is observed (Fig. 1 c,d); ii) if light is polarized perpendicularly to the plane of incidence (*s*-polarization) then *longitudinal contrast in transverse direction* is present (Fig. 1 b). In the latter cases of longitudinal contrasts, the in-plane domains with magnetization parallel to the plane of incidence can be distinguished, while the domains with magnetization in transverse direction occur to be equally gray. It is clearly seen in Fig. 2, where the contrast occurs only for the domains with in-plane magnetization, lying in the incidence plane (a-c) or for the domains with magnetization, pointing out of the sample plane in polar sensitivity (d). Besides, it should be mentioned, that the contribution from *polar* is always abundant in the total signal.

In the conventional setup (Fig. 1 e) with Köhler illumination path the LED or Xenon arc lamps are widely used and the angle of incidence, *i.e.* the sensitivity to the magnetization direction in the sample, is adjusted by the displaceable slit aperture, placed in a fully illumi-

nated aperture plane of the microscope, where in case of the crossed polarizer and analyzer the so called Maltese cross can be observed (Fig. 1). For the *polar* sensitivity the area in the middle of the conoscopic image has to be chosen (Fig. 1 a) and for *longitudinal* (plus *polar*) - one of the cross's arms (Fig. 1 b,c,d). When the only in-plane component of the magnetization is of the interest, those contribution have to be separated.

The separation is of great importance for the scientific community as such a possibility would extend the knowledge profit of the Kerr effect microscopy in many experimental issues: starting with domain observation in permanent magnets or other materials, where the magnetic anisotropy axes can be at a certain angle to the surface and, thus, the overlaid in-plane and out-of-plane domain structures may present^{12,13} [some other links?] ending with the interpreting of the experimental data itself¹⁴ and quantitative domain analysis, where the presence of both in-plane and polar contributions demand a careful calibration^{15,16}.

Another important issue is the magneto-optical contrast signal-to-noise ratio, that can be improved by a number of approaches: the use of the optimal analyzer-polarizer uncrossing angle^{1,9,17}; the difference-imaging technique¹¹ or normalized differential Kerr microscopy¹⁸. Anyway, for a certain materials with small Kerr rotation angles like Permalloy ($\text{Ni}_{19}\text{Fe}_{81}$)¹⁹ or thin films of diluted magnetic semiconductors^{8,20} those techniques may be not sufficient and further improvements are required.

As magnetic image processing requires some electro-magnet around the sample, the applied magnetic field can induce the parasitic Faraday effect (analogous to Kerr effect, but for the transmitted light)²¹ in lenses. Being orders stronger than Kerr effect it can notably influence the quality of the domain images⁸, bring an substantial errors into quantitative Kerr effect microscopy^{15,16} or lead even to misinterpreting of the experimental data¹⁴.

In this article we report on the development of a new hardware and software realization of the magneto-optical technique, which provides the opportunity for the selective Kerr microscopy *i.e.* to suppress the unwanted contrast contributions, remaining the desired components of the Kerr contrast: either in-plane or out-of-plane. An extra advantage of the reported technique is the suppression of the parasitic Faraday effect in lenses for the observation of domains in in-plane configuration. Another profitable outcome is the enhancement of the magneto-optical contrast signal-to-noise ratio by use of the improved difference-imaging technique. Moreover, the developed technique can be used as a basis for the new technical realization of the quantitative Kerr microscopy, discussed elsewhere [link vector Kerr paper](#).

II. SYSTEM DESIGN

The basic physical principle, which can be used for separation of the different Kerr contrasts is rather sim-

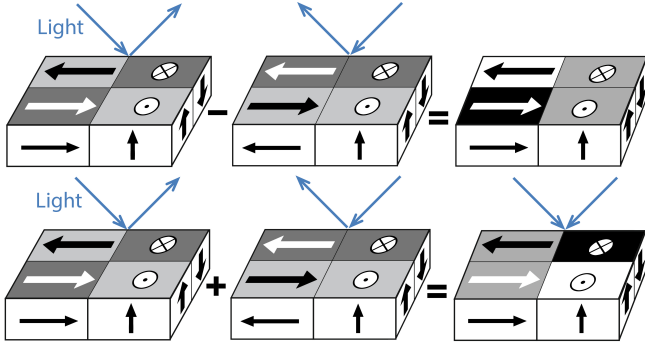


FIG. 3. The illustration of the contrast in the image of the magnetic sample, depending on the incident angle. For the inverted oblique light incidence the in-plane magnetization contrast is different, while the polar remains the same. Thus, by taking the difference between that two images the polar contrast can be eliminated **upper panel**. By combining both oblique light pathes (**lower panel**) the in-plane contrast can be suppressed. The arrows indicate the magnetization vector at the surface and the areal shading represents the Kerr contrast.

ple. From schematics in Fig. 1 (c,d) it is seen that when the direction of oblique light incidence is inverted the in-plane contrast is also inverted while the polar contrast remains unaffected. This is demonstrated in Fig. 2, where the contrast with the light coming from the left (Fig. 2 a) is opposite to that with the light coming from the right (Fig. 2 b). Thus, by taking the difference of the images with inverted light incidence the polar contrast can be eliminated (Fig. 3 (upper panel)). Such a Kerr contrast separation is possible only if the intensity of the light coming from the left and from the right are precisely equalized, otherwise, the out-of-plane component would not be completely compensated and undesirable polar contrast would occur. The bottle neck of the conventional setup for the opposite oblique incidences realization is the displaceable slit aperture, used to adjust the sensitivity (either longitudinal or polar). The mechanical adjustment brings a lot of instability to the optical system and the equalization of the light intensity is rather challenging or even hardly realizable at all. In developed system such a part, together with a common bulk light source were removed.

As a ground for the development the convectional Kerr-effect microscopy setup was used. It includes Zeiss wide-field polarization microscope with combined optical path (Fig. 1 e), CCD-camera (ORCA R2 by Hamamatsu), an in-plane or out-of-plane electromagnet and digital image processing software. For the realization of the selective Kerr effect microscopy a novel LED light source and the accomplishing measurement technique were developed. The light of eight ultra-high power LEDs is independently guided to the microscope via glass fibers (each 1 mm diameter) as shown in Fig. 4 e, whose ends are imaged to the back-focal plane and arranged together in a cross-like manner (Fig. 4 (c,d)). This corresponds

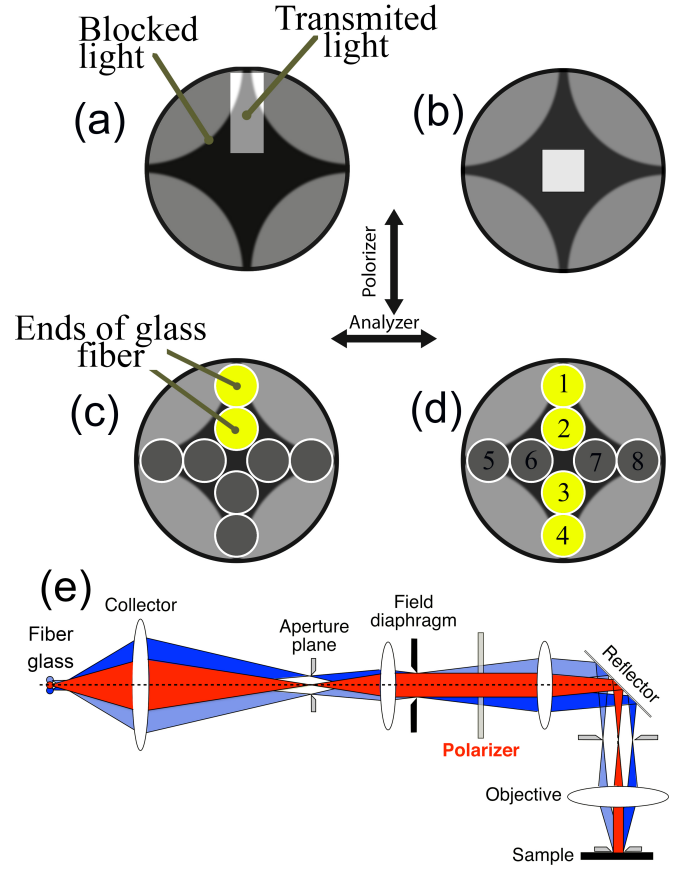


FIG. 4. The image of the conoscopic plane in conventional Kerr effect microscope (a,b) and a new developed one (c,d). The slit position in a fully illuminated aperture in conventional setup determines the sensitivity: longitudinal plus polar (a) or polar (b). The same sensitivity can be adjusted by turning on and off the appropriate LEDs, coupled to the glass fibers with their outputs, placed in aperture plane (c,d). The principle schema of the light path in a wide-field polarization microscope with combined optical path and fiber glass attached (e).

to eight virtual light sources directly in the conoscopic plane. Such an arrangement allows to set the incident angle for the oblique light only by turning ON and OFF the appropriate LEDs, without any mechanical action. Turning ON the LEDs 1&2 or 3&4 (Fig. 4 c) corresponds to the opening of the slit for the longitudinal (plus polar) sensitivity with *p-polarized* light in conventional microscope (Fig. 4 a), while 5&6 or 7&8 stand for the longitudinal (plus polar) sensitivity with *s-polarized* light.

After such an array of LEDs is introduced, the procedure for the suppression of the polar component of the contrast, based on the principle shown in Fig. 3 (upper panel) is straightforward: the LEDs have to be synchronized with camera and two sequential images with opposite incidence angle have to be taken and subtracted one from another as shown in Fig. 5: initially the LEDs 1&2 are switched ON and the first image is with a certain exposure time taken, then those two LEDs are turned

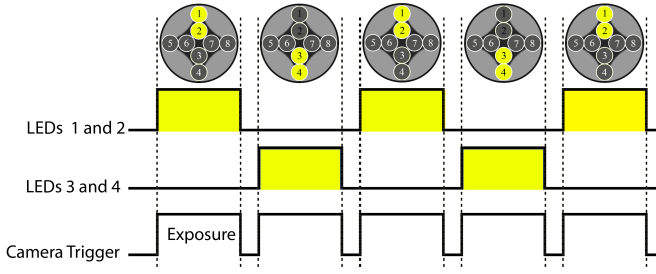


FIG. 5. Time diagram of the control sequence for the suppression of the polar contrast. The corresponding LEDs are switched ON and OFF synchronously with camera exposure time.

OFF and another pair of LEDs 3&4 is switched ON and the second image is taken. Afterwards, one image is subtracted from another and in resulting image only pure in-plane contrast is reserved.

As already mentioned, a special care has to be paid to the sample surface illumination. The intensity of the light coming from each of the complimentary groups of LEDs has to match, otherwise, the polar component would not be completely compensated leading to undesirable contrast in the domain image. For such an equalization, each of LEDs can be programmatically dimmed and with a feedback via the integral intensity of the realtime image they can be equalized.

In the developed light source there is no glass fiber output situated directly in the middle of the aperture plane, what would be equivalent to the open slit for the polar contrast as in Fig. 4 b. Alternatively, for the investigation of the out-of-plane magnetization component the combination of oppositely situated LEDs can be used. If LEDs 1,2&3,4 are ON, then for the symmetry reasons (Fig. 3 lower panel) the in-plane component is canceled, providing the *pure polar* contrast. As the Kerr rotation among other parameters is proportional to the overall light intensity other LEDs 5,6,7,8 can be switched ON to increase it. Alternatively, the inner circle of LEDs 2,3,6,7 can be used for high magnification objective lens.

III. EXPERIMENTAL RESULTS

A. Complimentary contrasts in Py film

First of all, the ability for the fast (within microseconds) switching of the LEDs provides an opportunity for the simultaneous observation of the domain structure in complimentary sensitivities. By synchronous triggering the LEDs and the camera as shown in Fig 6 (a), two consequently images of the same area of 40 nm thick Py film were taken: on in longitudinal sensitivities with the light coming from the top (b) and another with the light coming from the side (c), ensuring the 90° rotated sensitivity direction. As it is seen, if only one image with sensitivity along the cross-tie domain wall was considered,

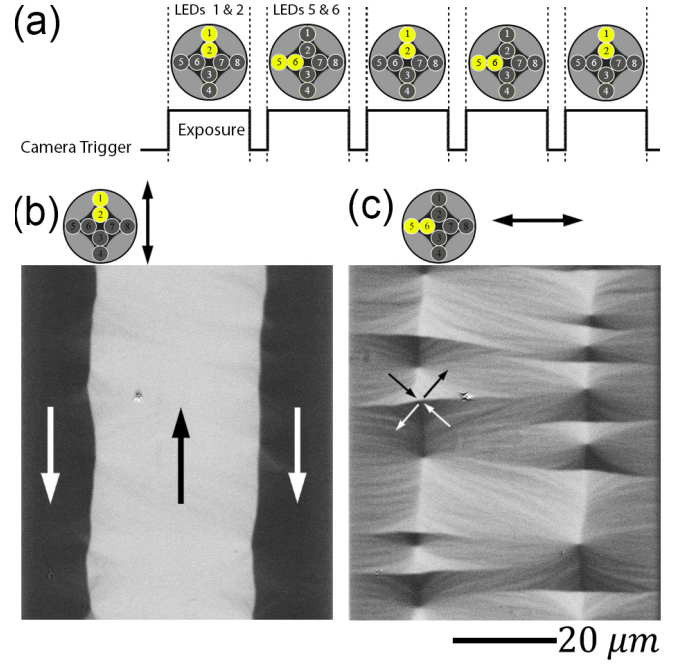


FIG. 6. **a**: time diagram of the control sequence for the simultaneous observation of the domain structure in complimentary sensitivities. **b,c**: domain wall in 40 nm thick $\text{Ni}_{81}\text{Fe}_{19}$ (permalloy) film in longitudinal sensitivity along the wall (**b**) and transverse to the wall (**c**). The cross-tie wall would not be observed if only the sensitivity along the wall was considered.

then the fine structure of the domain wall with transverse orientation of the magnetization, would be missed.

B. Contrast separation

The opportunity of the contrast selection in Kerr microscopy with use of the triggerable LED-based light is illustrated in Fig 7, where it was applied to the domain imaging in the sintered coarse-grained NdFeB polycrystal. The magnetization axes of the different grains are predominantly aligned in-plane with some small misalignment relative to the observed surface, *i.e.* each grain has a different component of the magnetization pointing out of the surface as schematically shown in Fig 7. Due to such an arrangement, in pure polar sensitivity the contrast between different grains can be observed (Fig 7 a). If the pure in-plane mode is applied, then after subtracting to images with opposite incidence no contrast between independent grains is observed, but the in-plane pattern, spreading throughout the whole sample including multiple grains, shows up (Fig 7 b).

Figure 8 shows a domain pattern in a cobalt bulk crystal, which has a uniaxial anisotropy at room temperature so that the easy axis is perpendicular to the observation surface. Thus, in polar sensitivity the flower pattern with a high degree of branching is observed (Fig. 8 a). In pure

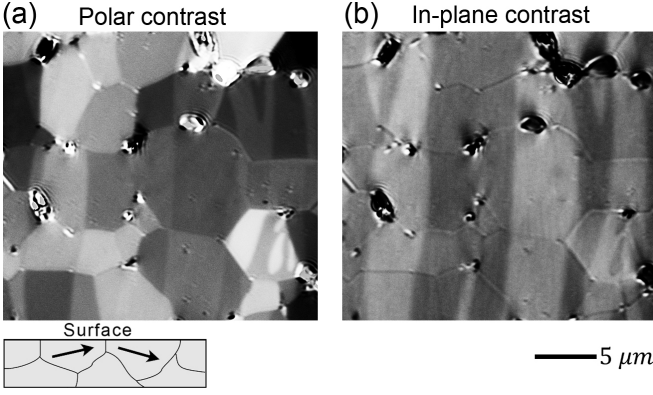


FIG. 7. Domains in a coarse-grained NdFeB sintered polycrystal, with separately imaged magnetization components perpendicular to the surface (a) and in-plane (b).

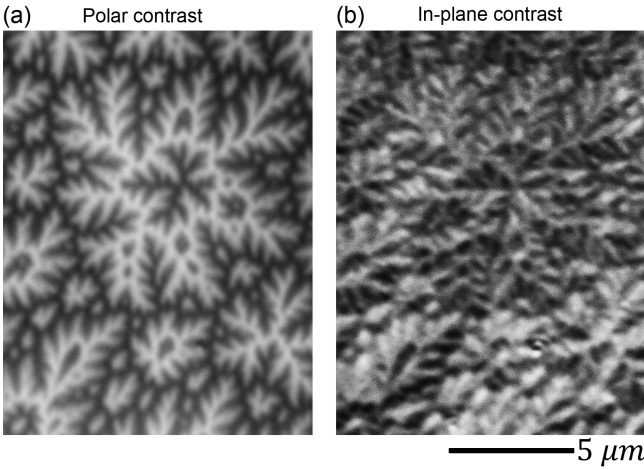


FIG. 8. Polar (a) and in-plane (b) magnetization components of a cobalt crystal cut parallel to the basal plane.

in-plane sensitivity the texture of the in-plane magnetization component, which had been made visible before only with electron polarization technique¹, is seen (Fig. 8 b). Since the polarized secondary electrons, in contrast to the magneto-optical imaging, see the magnetization in the very top nanometer of a sample the pure in-plane pattern in Fig. 8 (b) is strongly influenced by the magnetization variation within the material layer close to the surface.

C. Faraday effect correction and accuracy enhancement

In a conventional Kerr microscope, adjusted for the longitudinal Kerr effect, which is obtained at oblique light incidence by using a displaced shift aperture, there is always a superposition of in-plane and polar Kerr sensitivities together with a polar Faraday effect in the objective lens that is caused by polar magnetic fields in the objec-

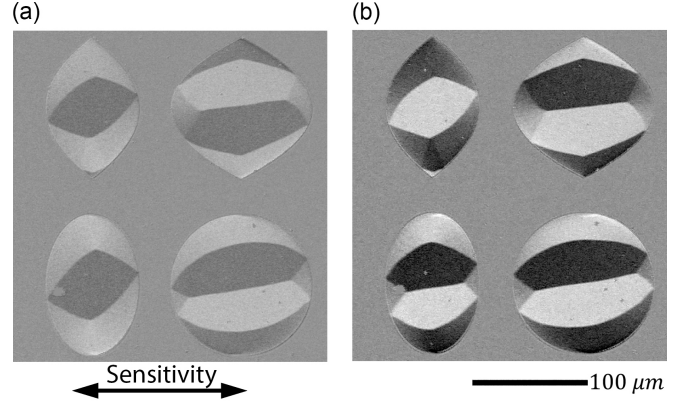


FIG. 9. Magnetic domains in $\text{Ni}_{81}\text{Fe}_{19}$ (permalloy) thin (240 nm) patterned film elements taken in longitudinal sensitivity with p-polarized light in conventional static mode (a) and pure in-plane (triggered) mode (b). In the latter case the contrast is doubled without any image post-treatment.

tive lens. In case of pure in-plane measurement in the triggered regime, also the parasitic out-of-plane Faraday effect in objective lens can be strongly suppressed. This parasitic contribution, being mostly linear with respect to the applied field in small fields, can, in principle, be eliminated by digital subtraction of the linear part but for a certain price in accuracy and sensitivity of the experiment. In some cases¹⁴ when this effect is caused by stray-fields of the sample itself it is highly non-linear and cannot be easily subtracted from the Kerr-signal coming from the sample. A hardware separation of Kerr- and Faraday effects is the only option then. As it is seen from Fig. 10 the in-plane optical hysteresis loop, measured in conventional mode (LEDs 1&2 are permanently on) (Fig. 10 b) with digitally subtracted Faraday effect (Fig. 10 c) is considerably noisy in comparison to that, measured with help of developed triggering technique (Fig. 10 f).

Besides this fortunate peculiarity to provide Faraday effect free-images, the triggered mode also provides a strong enhancement of the sensitivity of the instrument in pure in-plane mode, as the contrast for opposite oblique light is opposite, in difference image (Fig. 3 upper panel) it is doubled. It is nicely demonstrated in Fig. 9, where magnetic domain in Py patterned film elements are shown. The left image (a) is taken in conventional mode with statically illuminated sample in in longitudinal sensitivity with p-polarized light (LEDs 5&6 in Figure 4). The image to the right (b) is taken in pure in-plane mode with LEDs 5&6 and 7&8 been triggered (as shown in in Figure 5 for LEDs 1&2 and 3&4). It is clearly seen that the contrast for the latter image is strongly enhanced under the same experimental conditions (exposure time, camera gain, light intensity *etc.*) and without any image post-treatment.

Such an enhancement of the contrast increases the ultimate sensitivity of the measurement system. Figure 10

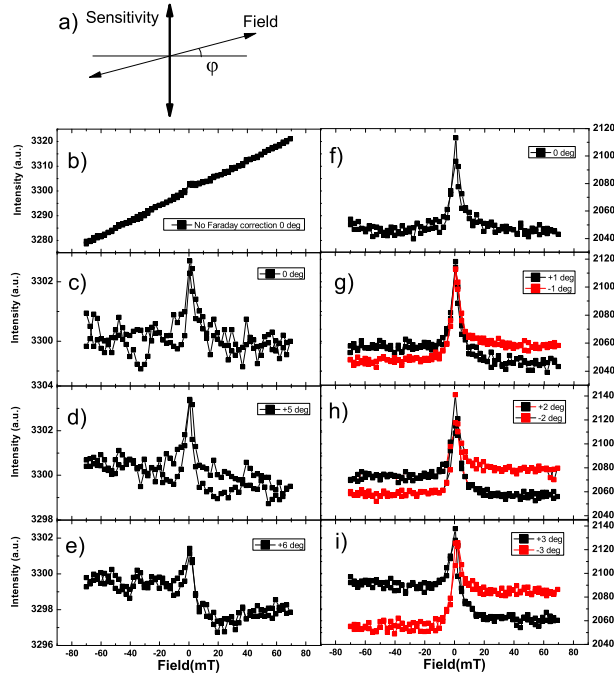


FIG. 10. The optical hysteresis loops made in conventional longitudinal plus polar mode (left panel) and in pure in-plane mode (right panel) in $\text{Ni}_{81}\text{Fe}_{19}$ 240 nm film. Loop taken before digital subtraction of the Faraday effect contribution (a) and after (b).

shows optical hysteresis loops, measured on a Py film in the conventional mode (left) and in the pure in-plane mode (right) without a compensator installed, i.e. ellipticity components in the reflected Kerr light are not compensated. In both cases the magnetic field was swept in-plane at an angle φ to the direction transversal to the sensitivity (see sketch in Fig. 10). At a field angle of 0° , no contrast between the saturated states is, thus, present. At a non-zero angle, the projection of the magnetization to the sensitivity direction is non-zero and as has different signs for positive and negative saturation states, so that a contrast between the saturated states will arise. As can be seen in Fig. 10 a, in the conventional mode the Faraday effect in the lenses overwhelms the whole magnetic response of the sample, and after digital subtracting (Fig. 10 b-d) the remaining Kerr signal occurs to be rather noisy. In this conventional Kerr mode a distinguishable contrast can be obtained only starting from field angles of $5 - 6^\circ$ (Fig. 10 c,d), while in the pure *in-plane* Kerr mode, due to the absence of the Faraday effect

contribution and the enhancement of the signal-to-noise ratio, a contrast can be observed already at $\varphi = 1^\circ$.

A quantitative estimation of the sensitivity can be obtained as follows. The longitudinal Kerr rotation angle as measured for Py in¹⁹ is $\phi_{Py} \approx 3 \cdot 10^{-4}$ radians or $30 \text{ mdeg} = 1.8'$. Then the detectable Kerr rotation is $2\phi_{Py}\sin(\varphi)$ ²². Thus for the conventional mode the minimal Kerr rotation, that can be clearly detected, is $\phi_{n.m.} = 2 \cdot 3 \cdot 10^{-4}\sin(5^\circ)$ radian $= 5.2 \cdot 10^{-5}$ radian $= 3 \text{ mdeg}$, and in the pure in-plane mode it is almost 5 times greater being as high as $\phi_{p.inp.m.} = 2 \cdot 3 \cdot 10^{-4}\sin(1^\circ)$ radian $= 1 \cdot 10^{-5}$ radian $= 0.6 \text{ mdeg}$.

IV. CONCLUSIONS

In this paper we have presented a novel hardware and software realization of the measurement technique for magneto-optical Kerr microscopy. The developed combination of the triggerable LED light source synchronized with the camera imaging provides the opportunity to separate contrast generated by in-plane and out-of-plane components of the surface magnetization *i.e.* selective Kerr microscopy. This technique was applied to investigation of the domain structure in a coarse-grained NdFeB sintered polycrystal and Cobalt single crystal and have demonstrated excellent results. In case of cobalt, pure in-plane texture of the in-plane magnetization component had been made visible for the first time by means of magneto-optical methods. The presented method also provides an enhancement of the in-plane contrast by a factor of 2 due to the extension of the conventional difference-imaging technique. Moreover, as in pure in-plane mode polar contrast contribution is suppressed, parasitic Faraday rotation, usually presented in conventional setup, is absent in this mode. Due to this fact and doubling of the contrast, the signal-to-noise ratio is drastically enhanced, what in its turn has strongly increased the sensitivity of the method. Finally, he developed technique can be used as a basis for the new technical realization of the quantitative Kerr microscopy.

Acknowledgement

????????????????

Notes

1. not to forget check pacs

¹ A. Hubert and R. Schäfer, "Magnetic domains: The analysis of magnetic microstructures," (Springer, New York, 1998) p. 696.

² W. Kuch, R. Schäfer, P. Fischer, and F. Hillebrecht, *Magnetic Microscopy of Layered Structures* (Springer, New York, 2015) p. 246.

- ³ A. Kehlberger, K. Richter, M. C. Onbasli, G. Jakob, D. H. Kim, T. Goto, C. A. Ross, G. Götz, G. Reiss, T. Kuschel, and M. Kläui, *Phys. Rev. Applied* **4**, 014008 (2015).
- ⁴ R. R. Gareev, V. Zbarsky, J. Landers, I. Soldatov, R. Schfer, M. Mnzenberg, H. Wende, and P. Grnberg, *Applied Physics Letters* **106**, 132408 (2015), <http://dx.doi.org/10.1063/1.4915323>.
- ⁵ F. Magnus, R. Moubah, U. B. Arnalds, V. Kapaklis, A. Brunner, R. Schäfer, G. Andersson, and B. Hjörvarsson, *Phys. Rev. B* **89**, 224420 (2014).
- ⁶ G. E. W. Bauer, E. Saitoh, and B. J. van Wees, *Nature Mater.* **11**, 391 (2012).
- ⁷ M. Weiler, M. Althammer, F. D. Czeschka, H. Huebl, M. S. Wagner, M. Opel, I.-M. Imort, G. Reiss, A. Thomas, R. Gross, and S. T. B. Goennenwein, *Phys. Rev. Lett.* **108**, 106602 (2012).
- ⁸ I. V. Soldatov, N. Panarina, C. Hess, L. Schultz, and R. Schäfer, *Phys. Rev. B* **90**, 104423 (2014).
- ⁹ J. McCord, *Journal of Physics D: Applied Physics* **48**, 333001 (2015).
- ¹⁰ R. Wayne, “Light and video microscopy,” (Elsevier, Netherlands, 2014) p. 368.
- ¹¹ F. Schmidt, W. Rave, and A. Hubert, *IEEE Transactions on Magnetism* **21**, 1596 (1985).
- ¹² O. Gutfleisch, D. Eckert, R. Schäfer, K. H. Müller, and V. Panchanathan, *Journal of Applied Physics* **87** (2000).
- ¹³ *The Fifth Symposium on Magnetism and Magnetic Materials: Recent Advancec in Magnetism and Magnetic Material (Taipei, Taiwan April 1989)* (World Scientific, Singapore, 1989).
- ¹⁴ D. Marko, I. Soldatov, M. Tekielak, and R. Schäfer, *Journal of Magnetism and Magnetic Materials* **396**, 9 (2015).
- ¹⁵ W. Rave, R. Schfer, and A. Hubert, *Journal of Magnetism and Magnetic Materials* **65**, 7 (1987).
- ¹⁶ W. Rave, P. Reichel, H. Brendel, M. Leicht, J. McCord, and A. Hubert, *Magnetism, IEEE Transactions on* **29**, 2551 (1993).
- ¹⁷ R. Schäfer, “Investigation of domains and dynamics of domain walls by the magneto-optical kerr-effect,” (John Wiley & Sons, Ltd, 2007).
- ¹⁸ J. McCord and A. Hubert, *physica status solidi (a)* **171**, 555 (1999).
- ¹⁹ T. Shun-ichi, *Japanese Journal of Applied Physics* **2**, 548 (1963).
- ²⁰ U. Welp, V. K. Vlasko-Vlasov, X. Liu, J. K. Furdyna, and T. Wojtowicz, *Phys. Rev. Lett.* **90**, 167206 (2003).
- ²¹ M. Faraday, *Phil. Trans. R. Soc. Lond.* **136**, 1 (1846).
- ²² *The factor 2 is due to the geometry of the experiment: the contrast is generated by two oppositely saturated states, which have positive and negative Kerr rotation angles, respectively.*